

Convergence in On-line Learning of Static and Dynamic Systems

Torbjörn Wigren

Ruoqi Zhang

Per Mattsson

Uppsala University, Department of Information Technology, P. O. Box 337, SE-75105, Sweden.

TORBJORN.WIGREN@IT.UU.SE

RUOQI.ZHANG@IT.UU.SE

PER.MATTSSON@IT.UU.SE

Abstract

The paper derives new conditions for global convergence of the adaptive moment generation algorithm when applied for on-line, or equivalently, recursive supervised learning of static and dynamic nonlinear systems. The paper also proposes a difference equation based nonlinear dynamic model, that enforces *structure* and results in a new type of recurrent neural network. The convergence analysis applies averaging using Ljung’s associated differential equation method. It is first proved that the asymptotic update behaviour of the adaptive moment generation algorithm is equivalent to a scaled stochastic gradient update for the standard hyper-parameter setting, or equivalent to a sign-sign update strategy in case the internal filtering of the algorithm is turned off. The analysis is concluded by proving global convergence to the set of parameters that gives a correct input-output description of the true system. The two hyper-parameter settings are evaluated with a Monte-Carlo analysis when the adaptive moment generation algorithm is applied for learning of nonlinear automotive cruise control dynamics. This validates the correct operation of the structured recurrent neural network and confirms the expected reduced convergence speed for the sign-sign update case.

Keywords: Adam, Associated ODE, Automotive Dynamics, Averaging, Convergence Analysis, Nonlinear Systems, Recurrent Neural Network, Recursive Identification, Supervised Learning.

1. Introduction

The adaptive moment generation algorithm (Adam) published by [Kingma and Ba \(2015\)](#) has become a workhorse in machine learning, with successful applications reported from a variety of fields. The majority of these applications concern static systems and batch processing. However, in the fields of adaptive control ([Åström and Wittenmark \(1989\)](#)) and recursive system identification ([Ljung and Söderström \(1983\)](#)), system dynamics is learned recursively and properties like stability ([Egardt \(1979\)](#); [Andersson et al. \(1986\)](#)) and convergence ([Ljung \(1977a\)](#); [Kushner and Clark \(1978\)](#)) become increasingly important as well as harder to achieve and analyse. The scope of this paper is therefore to have a renewed look on the convergence properties of Adam when used in a recursive setting for identification of nonlinear dynamic systems.

The fields of system identification and machine learning have overlapped increasingly in the last decade, due to an intensified focus on nonlinear dynamic systems, see [Pilonetti \(2013\)](#) and [Wigren et al. \(2022\)](#). From a system identification point of view, the neural network provides a parametrization that complements classical nonlinear model structures like piecewise linear static models ([Åström \(1985\)](#)), block oriented models ([Stoica and Söderström \(1982\)](#); [Westwick and Verhaegen \(1994\)](#)), the NARMAX class of models ([Chen and Billings \(1989\)](#)), as well as general state space models ([Schön and Gustafsson \(2003\)](#); [Wigren \(2005\)](#)). These model structures can all be used for recursive identification using the methods of [Ljung and Söderström \(1983\)](#). Some of the sequential Monte-Carlo (SMC) state space based algorithms ([Kantas et al. \(2015\)](#); [Schön et al. \(2015\)](#);

(Svensson and Schön (2017)) are not suitable for recursive identification due to inherent smoothing steps, however some algorithms like the bootstrap particle filter are, see e.g. Wigren et al. (2022). The machine learning field has avoided detailed dynamic nonlinear models in favour of general models like recurrent neural networks of various kinds (Prince (2023)) when addressing recursive identification applications. The advantage is generality, however this approach may overlook important impacts of the dynamics that may constrain the convergence of the algorithms themselves, cf. Ljung (1977b). In addition, neural networks lack the canonical model structures of the system identification field that minimize the set of parameters to avoid ambiguity, see Ljung and Söderström (1983), Söderström and Stoica (1989). Performance improvements are therefore expected when structure is enforced into neural network based models.

The paper by Kingma and Ba (2015) provides a first analysis of the convergence of Adam, with many later results following, e.g. Bock and Weiss (2019); Zou et al. (2019). In a recursive framework further results on convergence can be obtained by averaging analysis. In this paper the method with associated differential equations of Ljung (1975) is used. Briefly, the theorems of Ljung (1975) and Ljung (1977a) state how global stability of the associated ODE is related to global convergence of the algorithm, and how local stability of the ODE is related to local convergence.

The first contribution of the paper proposes a dynamic model that combines a discrete delay line chain and a static nonlinear function. When the nonlinear function is implemented with a neural network, structure is enforced in a new type of recurrent neural network (RNN). In the studied recursive identification setting another advantage is a complexity that is linear in the amount of data. The second contribution proves that for the typical hyper-parameter setting of Adam, the asymptotic average updating direction coincides with that of a diagonally power scaled stochastic gradient algorithm. Thirdly, when the internal filtering of Adam is turned off, the asymptotic average updating direction is proved to correspond to that of a sign-sign algorithm. The fourth contribution proceeds to prove that the algorithm converges to the set of parameters that give a perfect input-output description of the system. The final Monte-Carlo simulation study verifies the results by learning experiments of automotive cruise control dynamics. In particular the new RNN is shown to perform as expected.

The paper is organized as follows. Section 2 presents the structured RNN and lists the recursive version of Adam. Averaging tools are derived in Section 3 with the global convergence analysis appearing in Section 4. Numerical experiments and conclusions follow in Sections 5 and 6.

2. The Recursive Adaptive Moment Generation Algorithm

2.1. Model Structure

As a complement to existing RNNs, an approach that enforces structure by means of a canonical continuous time state space model is proposed here. The model signals are the multiple input signal vector $\mathbf{u}(t)$ consisting of K scalar signals, and the n -dimensional state vector $\hat{\mathbf{x}}(t, \boldsymbol{\theta})$ given by

$$\mathbf{u}(t) = (\mathbf{u}_1^T(t) \dots \mathbf{u}_K^T(t))^T \quad (1)$$

$$\mathbf{u}_k(t) = (u_k(t) \dots u_k^{(n_k)}(t))^T, \quad k = 1, \dots, K, \quad (2)$$

$$\hat{\mathbf{x}}(t, \boldsymbol{\theta}) = (\hat{x}_1(t, \boldsymbol{\theta}) \dots \hat{x}_n(t, \boldsymbol{\theta}))^T. \quad (3)$$

The superscript $^{(i)}$ denotes differentiation with respect to time, i times, to handle potential zero dynamics (Nijmeijer and v. Schaft (1990)), and $\boldsymbol{\theta}$ denotes the unknown parameter vector with dimension d . The ODE underpinning the model then follows as

$$\begin{pmatrix} \dot{\hat{x}}_1(t, \boldsymbol{\theta}) \\ \vdots \\ \dot{\hat{x}}_{n-1}(t, \boldsymbol{\theta}) \\ \dot{\hat{x}}_n(t, \boldsymbol{\theta}) \end{pmatrix} = \begin{pmatrix} \hat{x}_2(t, \boldsymbol{\theta}) \\ \vdots \\ \hat{x}_n(t, \boldsymbol{\theta}) \\ f(\hat{\mathbf{x}}(t, \boldsymbol{\theta}), \mathbf{u}(t), \boldsymbol{\theta}) \end{pmatrix}. \quad (4)$$

Here $f(\cdot, \cdot, \cdot)$ is a static single output smooth function that parameterizes the right hand side component of the ODE. When selected as a neural network $f^{nn}(\cdot, \cdot, \cdot)$ the end result will be an RNN, but it is stressed that $f(\cdot, \cdot, \cdot)$ is not restricted to that case. t denotes continuous time. Note that (4) is quite general since an arbitrary *vector* nonlinearity at the right hand side can be transformed to the structure of (4) using the inverse function theorem as explained in Nijmeijer and v. Schaft (1990).

An Euler method is then used to discretize (4) with sampling period T_S which results in

$$\begin{pmatrix} \hat{x}_1(t + T_S, \boldsymbol{\theta}) \\ \vdots \\ \hat{x}_{n-1}(t + T_S, \boldsymbol{\theta}) \\ \hat{x}_n(t + T_S, \boldsymbol{\theta}) \end{pmatrix} = \begin{pmatrix} \hat{x}_1(t, \boldsymbol{\theta}) \\ \vdots \\ \hat{x}_{n-1}(t, \boldsymbol{\theta}) \\ \hat{x}_n(t, \boldsymbol{\theta}) \end{pmatrix} + T_S \begin{pmatrix} \hat{x}_2(t, \boldsymbol{\theta}) \\ \vdots \\ \hat{x}_n(t, \boldsymbol{\theta}) \\ f(\hat{\mathbf{x}}(t, \boldsymbol{\theta}), \mathbf{u}(t), \boldsymbol{\theta}) \end{pmatrix}. \quad (5)$$

The p -dimensional output measurement model is assumed to be linear in the states, and given by

$$\hat{\mathbf{y}}(t, \boldsymbol{\theta}) = \mathbf{C}\hat{\mathbf{x}}(t, \boldsymbol{\theta}). \quad (6)$$

Here \mathbf{C} denotes the measurement matrix. In case n equals 0 a nonlinear static model results.

The parameterization of (5) is given by the details of $f(\hat{\mathbf{x}}(t, \boldsymbol{\theta}), \mathbf{u}(t), \boldsymbol{\theta})$, e.g. by the static neural network $f^{nn}(\hat{\mathbf{x}}(t, \boldsymbol{\theta}), \mathbf{u}(t), \boldsymbol{\theta})$ and its hyper-parameters. Noting that nowadays the gradient of the model $f(\hat{\mathbf{x}}(t, \boldsymbol{\theta}), \mathbf{u}(t), \boldsymbol{\theta})$ with respect to $\boldsymbol{\theta}$ is typically computed by auto-differentiation software at run-time, only the following high level definition of the gradient is needed

$$\boldsymbol{\psi}^\top(t, \boldsymbol{\theta}) = \frac{d\hat{\mathbf{y}}(t, \boldsymbol{\theta})}{d\boldsymbol{\theta}} = \mathbf{C} \frac{d\hat{\mathbf{x}}(t, \boldsymbol{\theta})}{d\boldsymbol{\theta}} = \mathbf{C}\boldsymbol{\Psi}(t, \boldsymbol{\theta}). \quad (7)$$

To obtain the matrix $\boldsymbol{\Psi}(t, \boldsymbol{\theta})$, the components of the difference equation (5) are formally differentiated with respect to $\boldsymbol{\theta}$. Exactly as in Wigren (2023) this gives the matrix difference equation

$$\begin{pmatrix} \frac{\partial \hat{x}_1(t+T_S, \boldsymbol{\theta})}{\partial \boldsymbol{\theta}} \\ \vdots \\ \frac{\partial \hat{x}_{n-1}(t+T_S, \boldsymbol{\theta})}{\partial \boldsymbol{\theta}} \\ \frac{\partial \hat{x}_n(t+T_S, \boldsymbol{\theta})}{\partial \boldsymbol{\theta}} \end{pmatrix} = \boldsymbol{\Psi}(t + T_S, \boldsymbol{\theta}) = \boldsymbol{\Psi}(t, \boldsymbol{\theta}) + T_S \begin{pmatrix} \frac{\partial \hat{x}_2(t, \boldsymbol{\theta})}{\partial \boldsymbol{\theta}} \\ \vdots \\ \frac{\partial \hat{x}_n(t, \boldsymbol{\theta})}{\partial \boldsymbol{\theta}} \\ \frac{\partial}{\partial \boldsymbol{\theta}} f(\hat{\mathbf{x}}(t, \boldsymbol{\theta}), \mathbf{u}(t), \boldsymbol{\theta}) \end{pmatrix}. \quad (8)$$

2.2. Algorithm

When the Adam algorithm is applied to (3)-(8) one may think that it would operate like any other recursive identification algorithm but there is a slight difference. This is because Adam does not process the gradient of the model separately, instead the full gradient of the criterion

$$V_A(\boldsymbol{\theta}) = \frac{1}{2} \lim_{t \rightarrow \infty} E[\boldsymbol{\varepsilon}^\top(t, \boldsymbol{\theta})\boldsymbol{\varepsilon}(t, \boldsymbol{\theta})] = \frac{1}{2} \lim_{t \rightarrow \infty} E[(\mathbf{y}(t) - \hat{\mathbf{y}}(t, \boldsymbol{\theta}))^\top (\mathbf{y}(t) - \hat{\mathbf{y}}(t, \boldsymbol{\theta}))] \quad (9)$$

is processed, where $\mathbf{y}(t)$ is the measurement. The gradient that is approximated by Adam is hence

$$\mathbf{g}(t, \boldsymbol{\theta}) = \left(\frac{dV_A(\boldsymbol{\theta})}{d\boldsymbol{\theta}} \right)^\top = - \lim_{t \rightarrow \infty} E[\boldsymbol{\psi}(t, \boldsymbol{\theta})\boldsymbol{\varepsilon}(t, \boldsymbol{\theta})]. \quad (10)$$

Hence, when Adam estimates approximate second order properties, this is done for $\boldsymbol{\psi}(t, \boldsymbol{\theta})\boldsymbol{\varepsilon}(t, \boldsymbol{\theta})$ rather than for $\boldsymbol{\psi}(t, \boldsymbol{\theta})$ that would be the case for a Gauss-Newton based recursive identification algorithm. This constrains the flexibility and has consequences that will be discussed in Section 4.

A recursive version of Adam is directly obtained from Algorithm 1 of [Kingma and Ba \(2015\)](#). It is then noted that the element-wise multiplication $\mathbf{g}(t) \odot \mathbf{g}(t)$ may be re-written as a vectorizing operation on the matrix $\mathbf{diag}(\boldsymbol{\psi}(t)\boldsymbol{\varepsilon}(t)\boldsymbol{\varepsilon}^\top(t))\boldsymbol{\psi}^\top(t)$. To describe the additional element-wise operations of Adam, a notation with a dot (\cdot) before the mathematical operation is used. When the operation is implicit like for multiplication, a single dot means element-wise operation.

After reordering equations to coincide with [Wigren \(2023\)](#) to facilitate the convergence analysis and replacing model signals with running estimates, the Adam algorithm becomes

$$\begin{aligned} \boldsymbol{\varepsilon}(t) &= \mathbf{y}(t) - \hat{\mathbf{y}}(t) \\ \mathbf{m}(t) &= \beta_1 \mathbf{m}(t - T_S) + (1 - \beta_1)(-\boldsymbol{\psi}(t)\boldsymbol{\varepsilon}(t)) \\ \hat{\mathbf{m}}(t) &= \frac{\mathbf{m}(t)}{1 - \beta_1^{\text{round}(t/T_S)}} \\ \mathbf{v}(t) &= \beta_2 \mathbf{v}(t - T_S) + (1 - \beta_2)(\mathbf{vec}(\mathbf{diag}(\boldsymbol{\psi}(t)\boldsymbol{\varepsilon}(t)\boldsymbol{\varepsilon}^\top(t)\boldsymbol{\psi}^\top(t)))) \\ \hat{\mathbf{v}}(t) &= \frac{\mathbf{v}(t)}{1 - \beta_2^{\text{round}(t/T_S)}} \\ \hat{\boldsymbol{\theta}}(t) &= \hat{\boldsymbol{\theta}}(t - T_S) - \alpha(t) \left(\hat{\mathbf{v}}^{\cdot \frac{1}{2}}(t) + \epsilon \right)^{-1} \cdot \hat{\mathbf{m}}(t) \\ \begin{pmatrix} \hat{x}_1(t + T_S) \\ \vdots \\ \hat{x}_{n-1}(t + T_S) \\ \hat{x}_n(t + T_S) \end{pmatrix} &= \begin{pmatrix} \hat{x}_1(t) \\ \vdots \\ \hat{x}_{n-1}(t) \\ \hat{x}_n(t) \end{pmatrix} + T_S \begin{pmatrix} \hat{x}_2(t) \\ \vdots \\ \hat{x}_n(t) \\ f(\hat{\mathbf{x}}(t), \mathbf{u}(t), \hat{\boldsymbol{\theta}}(t)) \end{pmatrix} \\ \hat{\mathbf{y}}(t + T_S) &= \mathbf{C}\hat{\mathbf{x}}(t + T_S) \\ \boldsymbol{\Psi}(t + T_S) &= \boldsymbol{\Psi}(t) + T_S \begin{pmatrix} \frac{\partial \hat{x}_2(t, \boldsymbol{\theta})}{\partial \boldsymbol{\theta}} \\ \vdots \\ \frac{\partial \hat{x}_n(t, \boldsymbol{\theta})}{\partial \boldsymbol{\theta}} \\ \text{autodiff}(f(\hat{\mathbf{x}}(t, \boldsymbol{\theta}), \mathbf{u}(t), \boldsymbol{\theta}), \boldsymbol{\theta}) \end{pmatrix} \Big|_{\boldsymbol{\theta}=\hat{\boldsymbol{\theta}}(t)} \\ \boldsymbol{\psi}(t + T_S) &= (\mathbf{C}\boldsymbol{\Psi}(t + T_S))^\top. \end{aligned} \quad (11)$$

Here $\mathbf{m}(t)$ denotes the first moment and $\hat{\mathbf{m}}(t)$ the bias corrected first moment, while $\mathbf{v}(t)$ and $\hat{\mathbf{v}}(t)$ denote the second (order) moments used to approximate a Newton search. β_1 and β_2 are filtering hyper-parameters and $\alpha(t) \propto t^{-1}$ is the gain sequence that needs to replace the constant step size α in the convergence analysis. $\mathbf{diag}(\cdot)$ extracts the diagonal matrix from a matrix and $\mathbf{vec}(\cdot)$ creates a vector of the diagonal elements.

3. Averaging Analysis

3.1. The Associated ODE and Convergence Relations

The results of [Ljung \(1975\)](#) and [Ljung \(1977a\)](#) replace the direct study of global convergence of (11), with a study of the global Lyapunov stability of the associated ODE of (11), which is defined

in terms of the average updating direction of (11). Provided that a Lyapunov function is found, then global convergence is implied by the results of Ljung (1975) and Ljung (1977a). The analysis below follows the Wigren (2023) closely by reference.

3.2. Conditions

The averaging analysis requires a number of regularity conditions to hold:

- M1: The model set $\mathcal{D}_{\mathcal{M}}$ is a compact subset of \mathcal{R}^d , such that $\boldsymbol{\theta} \in \mathcal{D}_{\mathcal{M}}$ implies that the state dynamics, the state gradient dynamics, and their derivatives are continuously differentiable, exponentially stable and bounded.
- M2: $\boldsymbol{\theta} \in \mathcal{D}_{\mathcal{M}}$ implies that $\mathbf{v}(t) > \delta_{\mathbf{v}} \mathbf{1}$, for some $\delta_{\mathbf{v}} > 0$.
- M3: $\mathbf{u}(t) = (u_1(t) \dots u_K(t))^{\top}$, without time derivatives, is generated from i.i.d bounded random vectors $\{\bar{\mathbf{u}}(t)\}$, by asymptotically stable linear filtering.
- G1: $\lim_{t \rightarrow \infty} t\alpha(t) = \bar{\alpha}$, $0 < \bar{\alpha} < \infty$.
- A1: The data $\{\mathbf{z}(t)\} = \{(\mathbf{y}^{\top}(t) \ \mathbf{u}^{\top}(t))^{\top}\}$ is strictly stationary and $\|\mathbf{z}(t)\| \leq C < \infty$, w.p.1, $\forall t$.
- A2: The average updating direction $\mathbf{f}(\boldsymbol{\theta}) = \lim_{t \rightarrow \infty} E \left[\left(\hat{\mathbf{v}}^{\frac{1}{2}}(t, \boldsymbol{\theta}) + \epsilon \right)^{-1} \cdot \hat{\mathbf{m}}(t, \boldsymbol{\theta}) \right]$ exists for $\boldsymbol{\theta} \in \mathcal{D}_{\mathcal{M}}$.
- S1: For each $t, s, t \geq s$, there exists a random vector $\mathbf{z}_s^0(t)$ that belongs to the σ -algebra generated by \mathbf{z}^t but is independent of \mathbf{z}^s (for $s = t$ take $\mathbf{z}_s^0(t) = \mathbf{0}$), such that $E[\|\mathbf{z}(t) - \mathbf{z}_s^0(t)\|^4] < C\lambda^{t-s}$, $C < \infty, |\lambda| < 1$.
- S2: The data generating system is described by $\mathbf{y}(t) = \mathbf{C}\mathbf{x}(t) + \mathbf{w}(t)$, where $\mathbf{x}(t)$ is generated by sampling of the states of a continuously differentiable, bounded and exponentially stable ODE, and where $\mathbf{w}(t)$ is generated from a sequence of i.i.d random vectors independent of $\{\mathbf{u}(t)\}$, by asymptotically stable filtering.

As in Wigren (2023) M1 - M3 defines a model set where exponential stability holds. M1 restricts the scope to continuously differentiable activation functions in case a neural network is used in (5) and (11). The conditions A1, S1 and S2 imply that also the data generating system is exponentially stable. With A2, the average updating direction is well defined and computable. The stochastic approximation condition G1 ensures an appropriate gain sequence decay rate. The use of the argument $(t, \boldsymbol{\theta})$ in A2 and below indicates the use of a *fix* value of $\boldsymbol{\theta}$ when expectations are computed.

3.3. The Convergence Analysis Tool

Since there is no projection algorithm defined for Adam the well known boundedness condition needs to be included, see Ljung (1975, 1977a) for a discussion:

The Boundedness Condition: There is a random variable C and an *infinite* subsequence $\{t_k\}$, such that $\hat{\boldsymbol{\theta}}(t_k) \in \bar{\mathcal{D}}_{\mathcal{M}} \subset \mathcal{D}_{\mathcal{M}} \setminus \partial\mathcal{D}_{\mathcal{M}}$ and with $\hat{\mathbf{x}}(t_k)$, $\boldsymbol{\Psi}(t_k)$, $\boldsymbol{\psi}(t_k)$, $\mathbf{x}(t_k)$, $\mathbf{u}(t_k)$, $\mathbf{w}(t_k)$ bounded by $C, \forall t_k$, w.p.1.

The following result then holds:

Theorem 1 Consider (11) and assume that M1-M3, G1, A1, A2, S1, S2 and the boundedness condition hold. Also assume that there exists a twice differentiable positive function $V(\boldsymbol{\theta})$ such that

$$\frac{d}{d\tau} V(\boldsymbol{\theta}_D(\tau)) \leq 0, \quad \boldsymbol{\theta}_D(\tau) \in \mathcal{D}_{\mathcal{M}} \setminus \partial\mathcal{D}_{\mathcal{M}},$$

when evaluated along solutions of the associated ODE

$$\frac{d}{d\tau}\boldsymbol{\theta}_D(\tau) = -\bar{\alpha}\mathbf{f}(\boldsymbol{\theta}_D(\tau)).$$

Then $\hat{\boldsymbol{\theta}}(t) \rightarrow \mathcal{D}_C = \{\boldsymbol{\theta}_D(\tau) \in \mathcal{D}_M \setminus \partial\mathcal{D}_M \mid \frac{d}{d\tau}V(\boldsymbol{\theta}_D(\tau)) = 0\}$ w.p.1, $t \rightarrow \infty$, or $\hat{\boldsymbol{\theta}}(t) \rightarrow \partial\mathcal{D}_M$.

Proof The proof parallels the proof of Theorem 1 of the downloadable open access paper [Wigren \(2023\)](#). Due to page constraints the present brief proof is given with reference to that publication. It is first proved that (11) can be written as the general algorithm of [Ljung \(1975\)](#). The regularity conditions M1-S2 are then proved to imply the corresponding conditions R1-R11 of [Ljung \(1975\)](#).

Algorithm Reformulation: The parameter, model, and gradient recursions of (11) fit the structure of the functions $\mathbf{Q}(\cdot, \cdot, \cdot)$ and $\mathbf{g}(\cdot; \cdot, \cdot, \cdot)$ of the general algorithm of [Ljung \(1975\)](#) listed as (A1) in [Wigren \(2023\)](#). A parallel mapping and time shift of the generalized states of (11), exactly as in the proof of Lemma 4 of [Wigren \(2023\)](#), then shows that (11) can be written as (A1).

Regularity Conditions: The verification of R1-R11 refers to the parallel proof of Lemma 5 of [Wigren \(2023\)](#) that is valid for a polynomial right hand side of (5). The boundedness of R1 follows from the stability of M1, and from M2, M3, A2 and S1, as in [Wigren \(2023\)](#). Addition of G1 to M1-M3, A2 and S1 allows verification of R2 by the same bounding of partial derivatives as in [Wigren \(2023\)](#), while the continuous differentiability of R3 follows by M1 and S2. The iterative bounding required to prove R4 is identical to the corresponding treatment of the polynomial case in [Wigren \(2023\)](#) since it is based on the continuous differentiability and exponential stability of M1 and S2, together with the boundedness of all driving signals that follows from M3, A1 and S2. R6 follows trivially from A2 since *the boundedness condition is assumed*. R7 follows from M3 and S2 since $\mathbf{u}(t)$ and $\mathbf{w}(t)$ are generated by filtering of i.i.d random vectors. R8-R11 are met since G1 holds. ■

4. Global Convergence

The global convergence of ADAM is then analysed for a first case with close to standard filtering, and a second case with filtering turned off. The analysis is performed assuming:

M4: The system and model are single output, i.e. $p = 1$.

4.1. The Scaled Stochastic Gradient Behaviour

The first case with close to standard filtering is defined by

A3: $\beta_2 \rightarrow 1$ and $\epsilon \rightarrow 0$.

To derive the asymptotic behaviour, the average updating direction of A2 is computed noting that the conditions M1-M3, A1, S1 and S2 imply strict asymptotic stationarity and ergodicity. To compute $\mathbf{f}(\boldsymbol{\theta})$, $(\hat{\mathbf{v}}(t, \boldsymbol{\theta})^{\frac{1}{2}} + \epsilon)^{-1}$ needs to be moved left of $E[\cdot]$ of $\mathbf{f}(\boldsymbol{\theta})$. This is the key step achieved by A3 and the fact that all filtering in (11) have static gains equal to 1. Then $\lim_{\beta_2 \rightarrow 1} \lim_{t \rightarrow \infty} \hat{\mathbf{v}}(t, \boldsymbol{\theta}) = \lim_{\beta_2 \rightarrow 1} \lim_{t \rightarrow \infty} \mathbf{v}(t, \boldsymbol{\theta}) = \lim_{t \rightarrow \infty} E[\mathbf{v}(t, \boldsymbol{\theta})] = \lim_{t \rightarrow \infty} E[\hat{\mathbf{v}}(t, \boldsymbol{\theta})]$ since the time constant of the filtering tends to infinity when $\beta_2 \rightarrow 1$. This gives

$$\lim_{\beta_2 \rightarrow 1} \lim_{t \rightarrow \infty} \hat{\mathbf{v}}(t, \boldsymbol{\theta}) = \lim_{t \rightarrow \infty} E \left[\epsilon^2(t, \boldsymbol{\theta}) \text{vec}(\text{diag}(\boldsymbol{\psi}(t, \boldsymbol{\theta})\boldsymbol{\psi}^\top(t, \boldsymbol{\theta}))) \right]. \quad (12)$$

Using A3 in the average updating direction of A2, and analysing the element-wise operations then allows the now non-stochastic part $\hat{\mathbf{v}}(t, \boldsymbol{\theta})^{-\frac{1}{2}}$ of (12) to be moved outside the expectation operator. The filtering of $\mathbf{m}(t)$ of (11) also disappears when taking expectations, hence

$$\lim_{\epsilon \rightarrow 0} \lim_{\beta_2 \rightarrow 1} \mathbf{f}(\boldsymbol{\theta}) = - \left(\lim_{t \rightarrow \infty} E \left[\varepsilon^2(t, \boldsymbol{\theta}) (\mathbf{diag}(\boldsymbol{\psi}(t, \boldsymbol{\theta}) \boldsymbol{\psi}^\top(t, \boldsymbol{\theta}))) \right] \right)^{-\frac{1}{2}} \lim_{t \rightarrow \infty} E [\boldsymbol{\psi}(t, \boldsymbol{\theta}) \varepsilon(t, \boldsymbol{\theta})], \quad (13)$$

where the diagonal matrix is positive definite by M2. [Ljung and Söderström \(1983\)](#) and (13) give:

Theorem 2 *Assume that M1-M4, A1-A3, S1 and S2 hold. Then the asymptotic behaviour of the parameter update of (11) coincides with the asymptotic parameter update of a stochastic gradient algorithm with diagonal power scaling.*

4.2. The Asymptotic Sign-Sign Behaviour

The average updating direction is then computed for the case with filtering turned off, assuming

$$\text{A4: } \beta_1 \rightarrow 0, \beta_2 \rightarrow 0 \text{ and } \epsilon \rightarrow 0.$$

The turned off filtering does not represent recommended hyper-parameters, but it enables an analytical derivation highlighting an asymptotic behaviour that is an indication of slow convergence.

Application of the limiting operations of A4 in the average updating direction of A2, and using the fact that $\varepsilon(t, \boldsymbol{\theta})$ is scalar by M4, gives

$$\begin{aligned} \lim_{\beta_1 \rightarrow 0} \lim_{\beta_2 \rightarrow 0} \lim_{\epsilon \rightarrow 0} \mathbf{f}(\boldsymbol{\theta}) &= - \lim_{t \rightarrow \infty} E \left[\frac{\varepsilon(t, \boldsymbol{\theta})}{\sqrt{(\varepsilon(t, \boldsymbol{\theta}))^2}} \left(\mathbf{vec}(\mathbf{diag}(\boldsymbol{\psi}(t, \boldsymbol{\theta}) \boldsymbol{\psi}^\top(t, \boldsymbol{\theta}))) \right)^{-\frac{1}{2}} \cdot \boldsymbol{\psi}(t, \boldsymbol{\theta}) \right] \\ &= - \lim_{t \rightarrow \infty} E [\mathbf{sign}(\varepsilon(t, \boldsymbol{\theta})) \mathbf{sign}(\cdot \boldsymbol{\psi}(t, \boldsymbol{\theta}))]. \end{aligned} \quad (14)$$

Again, note that a dot is used to denote element-wise operation. The result (14) is summarized in

Theorem 3 *Assume that M1-M4, A1, A2, A4, S1 and S2 hold. Then the asymptotic behaviour of the parameter update of (11) coincides with the asymptotic parameter update of a sign-sign algorithm.*

The reasons why a sign-sign behaviour is obtained is related to the fact that Adam adapts and normalizes the parameter update for the complete gradient $\boldsymbol{\psi}(t, \boldsymbol{\theta}) \varepsilon(t, \boldsymbol{\theta})$ in an element-wise way, contrary to Gauss-Newton algorithms ([Ljung and Söderström \(1983\)](#)). This can also be seen by a direct use of A4 in (11). Referring to [Dasgupta and Johnsson \(1986\)](#) and [Treichler et al. \(1987\)](#) it is well known that sign-sign schemes converge significantly slower than stochastic gradient algorithms.

4.3. Global Convergence - Common Part

The global convergence analysis of both cases above is based on the Lyapunov function candidate

$$V(\boldsymbol{\theta}) = V_A(\boldsymbol{\theta}) = \frac{1}{2} \lim_{t \rightarrow \infty} E[\varepsilon^2(t, \boldsymbol{\theta})] \geq 0. \quad (15)$$

In the SISO case of M4 and by use of M1-M4, G1, A1, A2, S1 and S2, the time derivative of the Lyapunov function along the solutions of the associated differential equation of Theorem 1 becomes

$$\begin{aligned}
 \frac{dV(\boldsymbol{\theta}_D(\tau))}{d\tau} &= \frac{d}{d\tau} \lim_{t \rightarrow \infty} \frac{1}{2} E [\varepsilon^2(t, \boldsymbol{\theta}_D(\tau))] = \lim_{t \rightarrow \infty} \frac{1}{2} E \left[\left(\frac{\partial \varepsilon^2(t, \boldsymbol{\theta})}{\partial \boldsymbol{\theta}} \right) \left(\frac{d\boldsymbol{\theta}_D(\tau)}{d\tau} \right) \right]_{|\boldsymbol{\theta}=\boldsymbol{\theta}_D(\tau)} \\
 &= \lim_{t \rightarrow \infty} E \left[\left(-\boldsymbol{\psi}^\top(t, \boldsymbol{\theta}) \varepsilon(t, \boldsymbol{\theta}) \right) (-\bar{\alpha} \mathbf{f}(\boldsymbol{\theta}_D(\tau))) \right]_{|\boldsymbol{\theta}=\boldsymbol{\theta}_D(\tau)} \\
 &= \bar{\alpha} \mathbf{f}^\top(\boldsymbol{\theta}_D(\tau)) \lim_{t \rightarrow \infty} E [\boldsymbol{\psi}(t, \boldsymbol{\theta}) \varepsilon(t, \boldsymbol{\theta})]_{|\boldsymbol{\theta}=\boldsymbol{\theta}_D(\tau)}. \tag{16}
 \end{aligned}$$

4.4. Global Convergence in the Scaled Stochastic Gradient Case

Proceeding from (16) and using (13) immediately gives

$$\begin{aligned}
 \frac{dV(\boldsymbol{\theta}_D(\tau))}{d\tau} &= -\bar{\alpha} \left(\lim_{t \rightarrow \infty} E [\boldsymbol{\psi}(t, \boldsymbol{\theta}) \varepsilon(t, \boldsymbol{\theta})] \right)_{|\boldsymbol{\theta}=\boldsymbol{\theta}_D(\tau)}^\top \\
 &\times \left(\lim_{t \rightarrow \infty} E \left[\varepsilon^2(t, \boldsymbol{\theta}) (\mathbf{diag}(\boldsymbol{\psi}(t, \boldsymbol{\theta}) \boldsymbol{\psi}^\top(t, \boldsymbol{\theta}))) \right] \right)_{|\boldsymbol{\theta}=\boldsymbol{\theta}_D(\tau)}^{-\frac{1}{2}} \lim_{t \rightarrow \infty} E [\boldsymbol{\psi}(t, \boldsymbol{\theta}) \varepsilon(t, \boldsymbol{\theta})]_{|\boldsymbol{\theta}=\boldsymbol{\theta}_D(\tau)} \leq 0. \tag{17}
 \end{aligned}$$

Equality holds if and only if $\lim_{t \rightarrow \infty} E [\boldsymbol{\psi}(t, \boldsymbol{\theta}) \varepsilon(t, \boldsymbol{\theta})] = 0$, referring to M2 and G1.

4.5. Global Convergence and the Symmetry Requirement in the Sign-Sign Case

Proceeding from (16) and using (14) results in

$$\begin{aligned}
 &\frac{dV(\boldsymbol{\theta}_D(\tau))}{d\tau} \\
 &= -\bar{\alpha} \lim_{t \rightarrow \infty} E \left[\mathbf{sign}(\varepsilon(t, \boldsymbol{\theta})) \mathbf{sign} \left(\boldsymbol{\psi}^\top(t, \boldsymbol{\theta}) \right) \right]_{|\boldsymbol{\theta}=\boldsymbol{\theta}_D(\tau)} \lim_{t \rightarrow \infty} E [\boldsymbol{\psi}(t, \boldsymbol{\theta}) \varepsilon(t, \boldsymbol{\theta})]_{|\boldsymbol{\theta}=\boldsymbol{\theta}_D(\tau)} \\
 &\quad - \bar{\alpha} \lim_{t \rightarrow \infty} E \left[\mathbf{sign}(\boldsymbol{\psi}(t, \boldsymbol{\theta}) \varepsilon(t, \boldsymbol{\theta})) \right]_{|\boldsymbol{\theta}=\boldsymbol{\theta}_D(\tau)}^\top \lim_{t \rightarrow \infty} E [\boldsymbol{\psi}(t, \boldsymbol{\theta}) \varepsilon(t, \boldsymbol{\theta})]_{|\boldsymbol{\theta}=\boldsymbol{\theta}_D(\tau)}. \tag{18}
 \end{aligned}$$

The following assumption is now introduced

A5: The distribution of the components of the stochastic vector variable $\boldsymbol{\psi}(t, \boldsymbol{\theta}) \varepsilon(t, \boldsymbol{\theta})$ are symmetric around their mean values when $t \rightarrow \infty$.

The reason why A5 is introduced is the following result:

Lemma 4 *Assume that the distribution p_X of the stochastic variable X is symmetric around its mean \bar{x} . Then $E[\mathbf{sign}(X)] = \mathbf{sign}(E[X])$.*

Proof

$$\begin{aligned}
 E[\text{sign}(X)] &= \int_{-\infty}^{\infty} \text{sign}(x)p_X(x)dx = \int_{-\infty}^0 (-1)p_X(x)dx + \int_0^{\infty} (1)p_X(x)dx \\
 &= \int_{-\infty}^{\infty} p_X(z + \bar{x})dz - \int_{-\infty}^{-\bar{x}} p_X(z + \bar{x})dz = \int_{-\bar{x}}^{\infty} p_X(z + \bar{x})dz.
 \end{aligned}$$

Noting that the integral is positive if $\bar{x} > 0$ and negative if $\bar{x} < 0$, Lemma 4 follows. \blacksquare

Referring to A5 and applying Lemma 4 element-wise, (18) becomes

$$\begin{aligned}
 \frac{dV(\boldsymbol{\theta}_D(\tau))}{d\tau} &= -\bar{\alpha} \mathbf{sign} \left(\lim_{t \rightarrow \infty} E \left[(\boldsymbol{\psi}(t, \boldsymbol{\theta}) \varepsilon(t, \boldsymbol{\theta}))^\top \right]_{|\boldsymbol{\theta}=\boldsymbol{\theta}_D(\tau)} \right) \lim_{t \rightarrow \infty} E[\boldsymbol{\psi}(t, \boldsymbol{\theta}) \varepsilon(t, \boldsymbol{\theta})]_{|\boldsymbol{\theta}=\boldsymbol{\theta}_D(\tau)} \\
 &= -\bar{\alpha} \sum_i \left| \lim_{t \rightarrow \infty} E[\boldsymbol{\psi}_i(t, \boldsymbol{\theta}) \varepsilon(t, \boldsymbol{\theta})]_{|\boldsymbol{\theta}=\boldsymbol{\theta}_D(\tau)} \right| \leq 0.
 \end{aligned} \tag{19}$$

Equality holds if and only if $\lim_{t \rightarrow \infty} E[\boldsymbol{\psi}(t, \boldsymbol{\theta}) \varepsilon(t, \boldsymbol{\theta})]_{|\boldsymbol{\theta}=\boldsymbol{\theta}_D(\tau)} = 0$.

4.6. Main Result

To state the main result the following final assumption is needed

S3: There exist parameter vectors $\boldsymbol{\theta}^*$ such that $y(t) = \hat{y}(t, \boldsymbol{\theta}^*) + \varepsilon(t, \boldsymbol{\theta}^*)$, where $\varepsilon(t, \boldsymbol{\theta}^*)$ is independent of $\mathbf{u}(t)$, with zero mean.

By S3, the condition $\lim_{t \rightarrow \infty} E[\boldsymbol{\psi}(t, \boldsymbol{\theta}) \varepsilon(t, \boldsymbol{\theta})]_{|\boldsymbol{\theta}=\boldsymbol{\theta}_D(\tau)} = 0$ holds for all $\boldsymbol{\theta}^*$ since $\boldsymbol{\psi}(t, \boldsymbol{\theta})$ is generated only from $\mathbf{u}(t)$ which is independent of $\varepsilon(t, \boldsymbol{\theta})$. This proves the main result

Theorem 5 *Assume that M1-M4, G1, A1, A2 and S1-S3 hold for (11). If i) A3 holds, or ii) A4 and A5 hold, then $\hat{\boldsymbol{\theta}}(t) \rightarrow \mathcal{D}_C$ w.p.1 as $t \rightarrow \infty$, or $\hat{\boldsymbol{\theta}}(t) \rightarrow \partial\mathcal{D}_M$, where $\boldsymbol{\theta}^* \in \mathcal{D}_C$.*

Convergence is global and Theorem 5 is valid for both cases treated by the paper. However there may be other sub-optimal classes of points in the invariant set \mathcal{D}_C than $\boldsymbol{\theta}^*$. Note that S3 implies that $w(t)$ of S2 can replace $\varepsilon(t, \boldsymbol{\theta}^*)$.

5. Numerical Results

To test the proposed RNN and to validate the results of the averaging analysis, a Monte-Carlo analysis of a simulated automotive cruise control system was performed. The vehicle traveling with velocity $x_1(t)$ is subject to thrust, friction, air resistance and gravitational forces in hilly terrain, see [Corona and DeSchutter \(2008\)](#); [Yueming and Zhiyuan \(2011\)](#); [Nilsson et al. \(2016\)](#). Here, the friction and gravitational forces are treated as a disturbance $w(t)$. Newton's second law gives

$$\dot{x}_1(t) = u(t) - \frac{\rho A C_{x_1}}{2m} x_1^2(t) - w(t), \tag{20}$$

In (20), $u(t)$ is the accelerator command, m the mass of the vehicle, A the frontal area, ρ the density of the air, and C_{x_1} is the air resistance coefficient. This system was sampled with $T_S = 0.1$ s. The

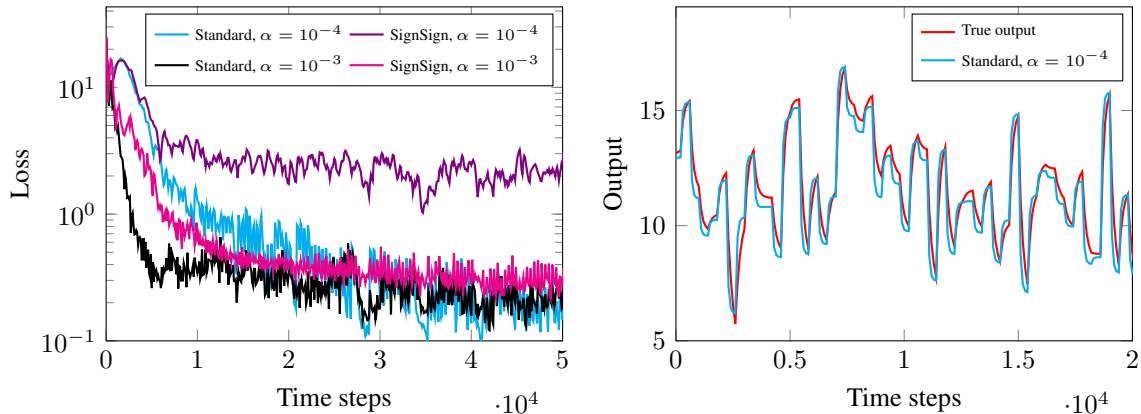


Figure 1: Convergence speeds of Adam (left). True and predicted output after training (right).

parameters were set similarly as in [Wigren and Teixeira \(2024\)](#). The white velocity measurement standard deviation was 0.1 m/s , while the standard deviation of the systems disturbance was 0.01 m/s^2 . To learn the system, $f^{nn}(\cdot, \cdot, \cdot)$ was selected with one hidden layer of width 8. A Python implementation was used to perform the Monte-Carlo analysis. The analysis averaged twenty runs for each of the two hyper-parameter settings analysed in Section 4, using the fix α values 0.001 and 0.0001. The \tanh activation functions was used. The results appear in Fig. 1 and they are consistent with the averaging analysis, with the standard hyper-parameter setting performing significantly better than the sign-sign case. The hyper-parameter setting resulting in a sign-sign algorithm with $\alpha = 0.0001$ appears to lead to very slow convergence. This may be due to the algorithm itself, that \mathcal{D}_C contains a suboptimal θ^* , or that A5 does not hold for the specific hyper-parameter setting.

6. Conclusions

The paper applied stochastic averaging analysis to a recursive Adam algorithm for two specific hyper-parameter settings. For these it was proved that Adam converges globally to the invariant set that is a superset of the parameter vectors that represent perfect input-output models. It was also proved that the setting that represents close to standard hyper-parameters behaves as a diagonally power scaled stochastic gradient algorithm, asymptotically in time. The case with hyper-parameters that turn off filtering behaves as a sign-sign algorithm, asymptotically in time. The latter case also *requires a non-standard symmetry condition* around the mean for the asymptotic update direction, to conclude on global convergence.

The proposed model structure of the paper lead to a structured RNN. A Monte-Carlo simulation study modeling automotive cruise control dynamics indicated that the new RNN performs as expected. Future research is however needed to fully characterize its performance envelope. In addition, the numerical study validated the theoretical analysis of Adam in terms of the adaptation speeds expected for the different hyper-parameter settings.

Acknowledgments

This work was supported by the Swedish Research Council (VR) under contract 2023-04546.

References

- B. D. O. Andersson, R. R. Bitmead, C. R. Johnsson Jr, P.V. Kokotovic, R. L. Kosut, I. M. Y. Mareels, L. Praly, and B. D. Riedle. *Stability of Adaptive Systems - Passivity and Averaging Analysis*. MIT Press, Cambridge, MA, 1986.
- K. J. Åström. *The adaptive nonlinear modeler*. Technical Report TFRT-3178, Department of Automatic Control, Lund Institute of Technology, Lund, Sweden, 1985.
- K. J. Åström and B. Wittenmark. *Adaptive Control*. Addison Wesley, Reading, MA, 1989.
- S. Bock and M. Weiss. A proof of local convergence for the Adam optimizer. Proc. IJCNN, 2019.
- S. Chen and S. A. Billings. Representation of nonlinear systems: The NARMAX model. *Int. J. Contr.*, 49:1013–1032, 1989.
- D. Corona and B. DeSchutter. Adaptive cruise control for a SMART car: a comparison benchmark for MPC-PWA control methods. *IEEE Trans. Contr. Systems Tech.*, 16, 2008.
- S. Dasgupta and C. R. Johnsson. Some comments on the behaviour of sign-sign adaptive identifiers. *System and Control Letters*, 7:75–82, 1986.
- B. Egardt. *Stability of Adaptive Controllers*. Lecture Notes in Control and Information Sciences, 159, 1979.
- A. Kantas, A. Docuet, S. S. Singh, J. Maciejowski, and N. Chopin. On particle methods for parameter estimation in state-space models. *Statist. Sci.*, 30:328–351, 2015.
- D. P. Kingma and J. Lei Ba. ADAM: A method for stochastic optimization. Proc. ICLR, San Diego, CA, USA, 2015.
- H. J. Kushner and D. S. Clark. *Stochastic Approximation Methods for Constrained and Unconstrained Systems*. Springer-Verlag, New York, NY, 1978.
- L. Ljung. *Theorems for the asymptotic analysis of recursive stochastic algorithms*. Report 7522, Department of Automatic Control, Lund Institute of Technology, Lund, Sweden, 1975.
- L. Ljung. Analysis of recursive stochastic algorithms. *IEEE Trans. Automat. Contr.*, AC–22:551–575, 1977a.
- L. Ljung. On positive real transfer functions and the convergence of some recursive schemes. *IEEE Trans. Automat. Contr.*, AC–22:539–551, 1977b.
- L. Ljung and T. Söderström. *Theory and Practice of Recursive Identification*. MIT Press, Cambridge, MA, 1983.
- H. Nijmeijer and A. J. v. Schaft. *Nonlinear Dynamic Control Systems*. Springer, New York, NY, 1990.
- P. Nilsson, O. Hussien, A. Balkan, Y. Chen, A. D. Ames, J. W. Grizzle, N. Ozay, H. Peng, and P. Tabuada. Correct-by-construction adaptive cruise control: two approaches. *IEEE Trans. Contr. Systems Tech.*, 24:1294–1307, 2016.

- G. Pilonetti. Consistent identification of Wiener systems: A machine learning viewpoint. *Automatica*, 49:2704–2712, 2013.
- S. J. D. Prince. *Understanding Deep Learning*. MIT Press, Boston, MA, 2023.
- T. Schön and F. Gustafsson. Particle filters for system identification of state-space models linear in either parameters or states. Proc. SYSID, pages 1251–2003, Rotterdam, the Netherlands, 2003.
- T. B. Schön, F. Lindsten, J. Dahlin, J. Wågberg, C. A. Naesseth, A. Svensson, and L. Dai. Sequential Monte-Carlo methods for system identification. Proc. SYSID, pages 775–786, Beijing, China, 2015.
- T. Söderström and P. Stoica. *System Identification*. Prentice–Hall International, Hemel Hempstead, UK, 1989.
- P. Stoica and T. Söderström. Instrumental-variable methods for identification of Hammerstein systems. *Int. J. Contr.*, 35:459–476, 1982.
- A. Svensson and T. B. Schön. A flexible state-space model for learning nonlinear dynamical systems. *Automatica*, 80:189–199, 2017.
- J. R. Treichler, C. R. Johnson, and M. G. Larimore. *Theory and Design of Adaptive Filters*. Wiley, New York, USA, 1987.
- D. Westwick and M. Verhaegen. Identifying MIMO Wiener systems using subspace model identification methods. *Signal Processing*, 52:235–258, 1994.
- A. Wigren, J. Wågberg, F. Lindsten, A. G. Wills, and T. B. Schön. Nonlinear system identification: Learning while respecting physical models using a sequential monte carlo method. *IEEE Control Systems Magazine*, 42:75–102, 2022.
- T. Wigren. Recursive identification based on nonlinear state space models applied to drum-boiler dynamics with nonlinear output equations. Proc. ACC, pages 5066–5072, Portland, Oregon, 2005.
- T. Wigren. Recursive identification of a nonlinear state space model. *Int. J. Adaptive Contr. Signal Processing*, 37:447–473, 2023. URL <https://onlinelibrary.wiley.com/doi/full/10.1002/acs.3531>.
- T. Wigren and A. Teixeira. Delay attack and detection in feedback linearized control systems. Proc. ECC, pages 1569–1576, Stockholm, Sweden, 2024.
- H. Yueming and L. Zhiyuan. An $\mathcal{H}_2/\mathcal{H}_\infty$ robust control approach to electric vehicle constant speed cruise. Proc. CDC, pages 2384–2389, Yantai, China, 2011.
- F. Zou, L. Chen, Z. Jie, W. Zhang, and W. Liu. A sufficient condition for convergences of Adam and RMSProp. Proc. CVPR, pages 11119–11127, 2019.